Aalborg Universitet

AALBORG UNIVERSITY

DENMARK

Robust Decentralized Cooperative Resource Allocation for High-Dense Robotic Swarms by Reducing Control Signaling Impact

Morejon, Santiago; Bruun, Rasmus; Fernandes, Filipa Santana da Silva; Sørensen, Troels Bundgaard; Kiilerich Pratas, Nuno; Madsen, Tatiana Kozlova; E. Mogensen, Preben

Link to publication from Aalborg University

RESEARCH ARTICLE

Robust Decentralized Cooperative Resource Allocation for High-Dense Robotic Swarms by Reducing Control Signaling Impact

C. SANTIAGO MOREJÓN GARCÍA[1], (Member, IEEE), **RASMUS LIBORIUS BRUUN**[1],
FILIPA S. S. FERNANDES[1], (Member, IEEE), **TROELS B. SØRENSEN**[1], **NUNO K. PRATAS**[2],
TATIANA KOZLOVA MADSEN[1], **AND PREBEN MOGENSEN**[1,2]
[1]Wireless Communication Networks Section, Department of Electronic Systems, Aalborg University, 9220 Aalborg, Denmark
[2]Nokia Standards, 9220 Aalborg, Denmark

Corresponding author: C. Santiago Morejón García (csmg@es.aau.dk)

ABSTRACT High throughput, low latency, and high reliability in proximity communications for swarm robotics can be achieved using decentralized cooperative resource allocation schemes. These cooperative schemes minimize the occurrence of half-duplex problems, reduce interference, and allow a significant increase in the achievable swarm density, but requires additional signaling overhead, which makes them potentially more prone to performance degradation under realistic operation conditions. These conditions include both data, signaling, and their interdependence evaluated jointly. The negative impact of the signaling errors requires incorporating enhancement techniques to realize the full potential of the cooperative schemes. Particularly, in this paper and for this purpose, we evaluate the effects of hybrid automatic repeat request (HARQ), link adaptation by aggregation (LAAG) and beam selection by using directional antennas in the cooperative schemes, and compare performance with 3rd Generation Partnership Project (3GPP) NR sidelink mode 2 (including signaling) using the same techniques. Additionally, we include a comparison of the required number of control signals between sidelink mode 2 inter-UE coordination (IUC) and cooperative schemes, and introduce a decentralized rebel sub-mode behavior in our group scheduling scheme to further improve the performance at the 99.99 percentile. The simultaneous use of all these enhancement techniques in our cooperative schemes considerably reduces the impact of signaling errors and thereby increases the supported swarm size compared to sidelink mode 2.

INDEX TERMS Cooperative communication, distributed resource allocation, swarm communication, beam selection, antenna directivity.

I. INTRODUCTION

Industrial factories' production of goods is changing thanks to the fourth industrial revolution (I4.0). It aims to change the traditional linear, sequential, and centralized production, which lacks flexibility and reconfiguration capabilities [1]. A swarm-based production, based on simple agents collaborating between them, can perform the same task as a highly specialized one [2] and add more flexibility for increased efficiency. To perform the tasks (e.g., manufacturing tasks

The associate editor coordinating the review of this manuscript and approving it for publication was Eyuphan Bulut.

or enabling production flows), either production robots or autonomous mobile robots (AMR) can be used [3], turning factories into an unstructured environment with manufacturing systems and routing of goods changing dynamically [4]. automated guided vehicle (AGV) is an example of efficient warehouse systems where humans are either replaced by robots or collaborate closely with them [5]. The use cases above set new requirements for communication technologies with higher throughput, lower latency, and higher reliability than current wireless systems can offer [6], [7], [8]. Besides the challenges from radio propagation effects in industrial environments, causing outages for wirelessly

commuted robots [9]. Their displacement across a large factory produces frequent handovers or link breakage due to uncovered areas [9], increasing latency and affecting the communication's reliability. Reliability is directly linked to latency since it can be defined as the receiver's successful reception probability within the application's latency requirement. device-to-device (D2D) communication represents a suitable option to fulfill the new requirements by overcoming the problems mentioned above and providing connectivity in places where the network's coverage does not reach or where there are frequent handovers [9]. It provides one-hop communication improving the overall network capacity [10], spectrum and energy efficiency, and reducing transmission latency [11]. D2D deployed in the licensed spectrum can attain quality of service (QoS), reflected on controlled interference, better energy consumption rate, and better spectrum utilization, in comparison to unlicensed bands which are unregulated and uncoordinated irrespective of network traffic increment [10], [12], [13], [14]. For the licensed spectrum, 3GPP supports two sidelink-transmission modes for D2D. They consist in allocating time-frequency resources for D2D links, either by devices having the network's assistance (i.e., sidelink mode 1 [15]) or by doing it autonomously (i.e., sidelink mode 2 [15]). We will use sidelink mode 2 (mode 2) as a reference in our study, and assume the same basic procedures for our cooperative schemes. Section II explains in more detail mode 2.

A. RELATED WORK

Our main focus is on the data exchange or communication, between robots, and how to allocate resources for their transmissions subject to given constraints. Robots move around the facility to perform different tasks through having a collective perception of the environment. Data exchange considers stringent communication requirements by means of high throughput at 10 Mbps with a maximum latency of 10 ms and 99.99% reliability [16]. In our previous work, we proposed the incorporation of cooperative capabilities into the resource allocation by following two approaches [17]. The first one uses a priority-based sequential order to allocate resources among robots in need to exchange data. It is denoted as a device sequential scheme. The second one considers the formation of groups among robots where they designate one as a group leader in charge of allocating resources for itself and all group members. It is named group scheduling scheme. Section III explains both schemes in more detail. In [18] we formulated the optimization problem of determining the resource allocation matrix $\mathbf{A}_{N_r \times S_l}$, where N_r corresponds to the maximum number of robots that can be supported in the swarm and S_l to the set of time slots that spans the swarm's allocation period. This problem, i.e., trying to determine an allocation supporting the maximum number of robots subject to interference constraints that guarantee throughput and latency, is an NP-hard problem [19]. Instead, we use heuristic methods to efficiently determine the sub-optimal solutions

to decentralized resource allocation by using cooperative resource allocation.

The design of the control signaling for the cooperative resource allocation was evaluated by using the failure probability key performance indicator (KPI) (i.e., probability of unsuccessful reception of a 100 kbit message within 10 ms latency). The results showed that a swarm size of ten robots just met the 10^{-4} failure probability (equivalent to 99.99% reliability) requirement when using the device sequential scheme; increasing the swarm size further requires enhancing techniques. One highly used technique is hybrid automatic repeat request HARQ which was introduced by 3GPP in [20] and adopted within the standard in high speed packet access (HSPA), release 7 [21], [22]. Another well known and utilized technique by 3GPP is link adaptation [23] which is based on outer loop power control (OLPC) [24]. Our approach uses link adaptation by allocating additional time-frequency resources, denoted as link adaptation by aggregation (LAAG), to add robustness. Incorporating both techniques [25] allowed to increase the swarm size up to twenty, forty, and fifty robots when using mode 2, group scheduling, and device sequential, respectively. Further increase in the swarm size needs techniques to handle interference due to half-duplex problems, where communication is attempted on the same resources (when robots exchange data) and uncoordinated transmissions when they do not.

One approach that could further enhance the solution put forward in this paper would be the application of network coding principles [26], [27]. For example, upon receiving the transmitted packets of the surrounding peer robots, a robot could perform a re-transmission where it would combine (e.g., apply an XOR) these different packets and potentially its packet. This would allow the surrounding robots that could not receive some of the packets to recover these. However, this type of solution can require multiple re-transmissions and tight coordination between the robots. Therefore, achieving all this within the tight deadline of the targeted setting would be challenging. So the inclusion of network coding principles has been left for future work.

On the other hand, directional antennas and beam selection represent a suitable technique for our use case since it minimizes the detrimental effects of half-duplex problems and generally improves the signal-to-noise-plus-interference ratio (SINR). For example, directional antennas equipped in a unmanned aerial vehicle (UAV) [28], unmanned ground vehicle (UGV) [29], or a car [30] reduced the number of handovers, achieve a robust long-range communication link, or increase the reference signal received power (RSRP) and reference signal received quality (RSRQ), respectively.

B. CONTRIBUTIONS AND PAPER ORGANIZATION

We have seen the benefit of cooperative resource allocation schemes over mode 2 [17], [18], HARQ and LAAG applied to mode 2 and cooperative schemes [25], and directional antennas to mode 2 [31] knowing that interference is a limiting factor for D2D. In order to increase swarm sizes
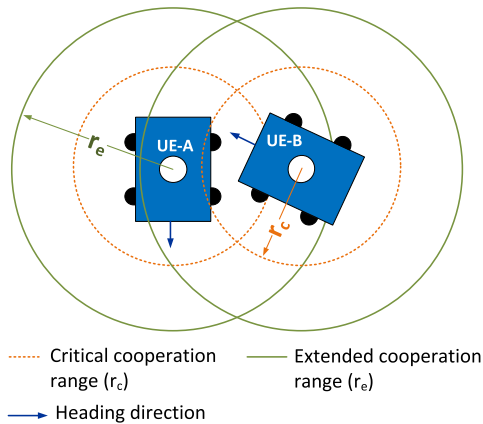
FIGURE 1. Two UE-centric proximity ranges to exchange discovery messages (r_e) and data (r_c).

further in this paper, we show how our proposed cooperative schemes can benefit from the same enhancement techniques and outperform mode 2 when directional antennas and beam selection are used to reduce interference. Specifically, our contributions are:

— Review of mode 2 and our cooperative schemes, with detailed explanations of the enhancement techniques.
— Comparison of the number of required control signaling messages to achieve coordinated/cooperative resource allocation between mode 2 IUC and cooperative schemes.
— Demonstrating the superiority of device sequential and group scheduling over mode 2.
— Detailed analysis of how HARQ, LAAG, and beam selection impact the failure probability.
— Enhancement of the group scheduling scheme compared to [25] that improves failure probability at 99.99 percentile.

The rest of this paper is organized as follows: Section II introduces our use case and provides an explicit characterization of mode 2. The explanation extends to our proposed cooperative resource allocation schemes in Section III. Section IV presents the HARQ and link adaptation as well as our system design for directional antennas and beam selection and its applicability for device sequential and group scheduling. Section V outlines the simulation setup, followed by results and an evaluation of them in Section VI. Finally, conclusions, final remarks, and future work are presented in Section VII.

II. 3GPP 5G NR SIDELINK MODE 2
Our use case contemplates the deployment of a swarm of robots within a rectangular indoor factory to perform several tasks. They move at a constant speed between random waypoints uniformly and randomly placed across the factory. Each robot incorporates a UE to transmit and receive data to/from other pairs. Since the focus of our studies is on D2D communication, there is no route planning and

collision avoidance, meaning that robots can pass through each other [17].

Data exchange occurs when robots are close to each other, i.e., within *critical cooperation range* r_c (orange dotted circle in Fig. 1). Robots identify the presence of others within r_c by acquiring the knowledge of their position and heading direction when exchanging *discovery messages* (DMs) within *extended cooperation range* r_e (green circle in Fig. 1). It is larger than r_c ($r_e > r_c$).

Data and discovery information are generated semi-persistently (i.e., robots generate new data after a predefined period) using a simplified model [32]. Therefore, we assume the absence of non-semi-persistent transmission (SPS) traffic. For simplicity, we adopt no misalignment in data generation, contrarily to [33]. We assume that data and discovery messages are exchanged in different resource pools.

Focusing on data transmissions, mode 2 requires UEs to follow two procedures: **sensing** and **NR slot selection**.

A. SENSING
UEs monitor the channel for a preconfigured period defined as *sensing window*. It can have a maximum value of one-second [15] across the configured bandwidth. The monitoring consists of determining the set of candidate time-frequency NR slots through the sidelink control indicator (SCI) reception. The objective is to determine if a slot is suitable for the UE data transmission. Therefore, two parameters need to be evaluated. The first one is the *"resource reservation period"*, which, if present, indicates that the slot is being utilized by other UE's SPS. The second one is the RSRP. It indicates if the received signal's power is sufficiently high to be considered interference depending on whether it is above or below a predefined threshold. If the set of candidate slots does not meet the 20% of the total within the sensing window, the predefined RSRP value increases by 3dB to re-evaluate until reaching 20%.

B. NR SLOT SELECTION
Once the set of candidate slots is obtained, the UE determines the number of slots required for its data transmission. Then, the slot selection proceeds either *uncoordinated* or *coordinated*.

1) UNCOORDINATED NR SLOT SELECTION
A UE randomly selects the number of required slots among the ones in the set. Since the UE traffic is periodic, an SPS transmission is performed in the selected slot(s). The time the UE holds the slot(s) reservation is determined by the re-selection counter [34]. A drawback of this scheme is the potential presence of half-duplex problems (i.e., UEs choosing the same slot(s), making it impossible for simultaneous transmission and reception of data) due to the randomness in the process. A full overlap of slots happens when all required selections match; otherwise, it is a partial overlap. In [35], the authors propose a solution to tackle this kind of issue. They described and analyzed the probability that a vehicle losses
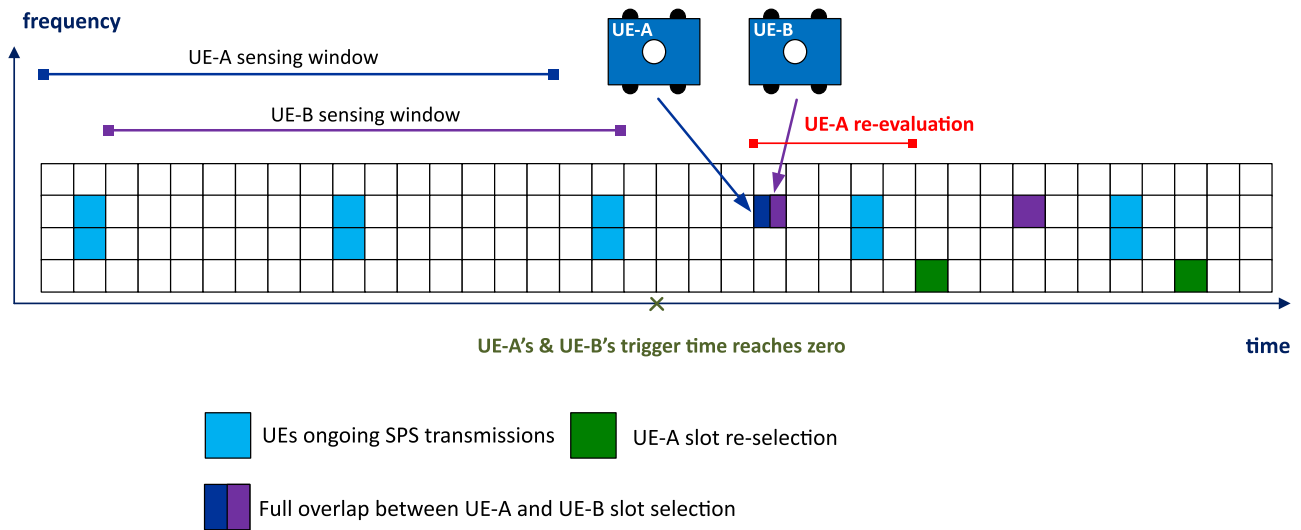
FIGURE 2. Uncoordinated NR slot selection followed by re-evaluation procedure by UE-A to re-select a slot after noticing a half-duplex occurred with UE-B selection.

several consecutive collision avoidance message (CAM)s from one of its neighbors and proposed an extension to long term evolution (LTE) sidelink mode 4, which significantly alleviated it. However, CAMs carry a significantly smaller amount of data compared to our use case. Moreover, 3GPP recently introduced a re-evaluation feature in release 17 [36] to reduce the half-duplex impact on performance. It contemplates the sensing and checking of SPS transmissions and UE's previous reserved slot(s). It occurs within a predefined amount of slots. It allows UEs to evaluate their selection and make a new one if half-duplex problems occur. Executing a re-evaluation and re-selection may also impact latency, as it is not guaranteed the absence of half-duplex problems. Fig. 2 illustrates the UE-A's re-selection procedure when it detects a full overlap (one slot required) with UE-B.

2) COORDINATED NR SLOT SELECTION

It is known as inter-UE coordination (IUC) and was introduced in 3GPP release 17 [36]. It consists of two schemes that allow coordinated slots selection to avoid half-duplex problems. They were named as *scheme 1* and *scheme 2*. *Scheme 1* consists of sharing the set of preferred or non-preferred slots after a IUC trigger (e.g., UE-B needing to know which resources to use to reach UE-A successfully) occurs. It can be either a transmitter's IUC explicit request received by the receiver (i.e., option 1) or other conditions (i.e., option 2), for example, SCI request or higher-layer signaling. *Scheme 2* contemplates transmitter UE indicating the selected slots for its transmission in the SCI. The receiver UE indicates the expected/potential conflicts on that slot(s) selection such that the transmitter UE can perform a slot(s) re-selection. IUC entails the use of transmissions for IUC trigger/IUC information. In our use case, enabling IUC will create a more congested resource pool in addition to the
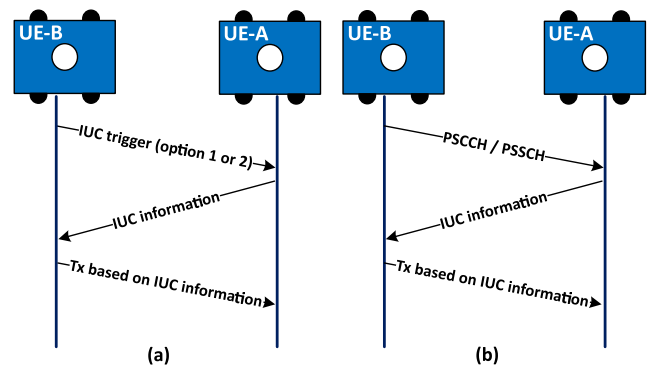

FIGURE 3. Coordinated NR slot selection through IUC schemes 1 & 2 between two UEs.

potential presence of half-duplex problems and interference (i.e., UEs transmitting in the same slot but not intending to exchange information). Fig. 3 shows IUC between UE-A and UE-B by using *scheme 1* (a) or *scheme 2* (b).

The latest mode 2 in 3GPP release 17 has proved that coordination among UEs resource allocation is the key to increasing its performance. Since IUC messages are exchanged between a pair of UEs, applying it to our use case represents that UEs require the exchange of a lot of IUC messages among their relatives located within r_c. Unfortunately, the design does not contemplate using only one IUC message for a whole group of UEs. Additionally, as coordination is not free-granted, having a more congested resource pool is the price. For that reason, our decentralized resource allocations schemes in [17] represent a suitable option for this use case since they are based on mode 2's design.

III. COOPERATIVE RESOURCE ALLOCATION SCHEMES

Cooperative resource allocation schemes were designed to achieve the most likely usage of all available slots by
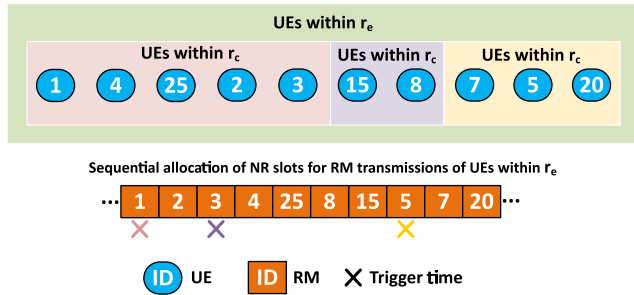
FIGURE 4. Resource allocation by using device sequential scheme for devices within r_c and r_e.

FIGURE 5. Resource allocation by using group scheduling scheme for devices within r_c and/or r_e.

exchanging the least possible cooperative message signaling. It is achievable by determining: who (which UE performs the resource allocation), when, and what information is required for those decisions.

Cooperation requires the use of a new control signal in addition to the *discovery message* (DM) that includes UE's coordinates and heading direction [18]. It is denoted as *resource selection message* (RM) and contains information about the selection of resources a UE made for its data transmission. Then, to answer the questions posed, we proposed the inclusion of the *trigger time* parameter in the DMs. Trigger time is the time estimated by a UE when another will be within its r_c or when the re-selection counter reaches zero to proceed with the selection of resources. Once the selection is made, this information is shared in the RMs to all UEs within r_e. Our proposal considers performing the resource allocation in sequential order or by a group leader. For the latter, the incorporation of the *leader selection* parameter is required in DMs. We named these two approaches as ***device sequential*** and ***group scheduling*** schemes respectively.

A. DEVICE SEQUENTIAL SCHEME

This scheme contemplates UEs prioritizing their slot selection by evaluating in the first place the trigger time since it determines which UE(s) has a higher priority to allocate slot(s). If several UEs coincide with their trigger time, they place the priority order by following the sequential order of their unique IDs. In this case, the lower unique ID represents a higher priority. In our example in Fig. 4, all UEs have the same r_e such that they exchange DMs (green box). The colored boxes (pink, purple, and yellow) indicate the group of UEs having the same trigger time, while the colored crosses indicate the exact time the resource allocation needs to occur (i.e., RMs need to be transmitted). The earliest trigger time is for UEs 1, 4, 25, 2, and 3. They follow the sequential order for slot selection 1, 2, 3, 4, and 25. UEs' 8 and 15 trigger time falls in the same slot UE 4 performs its allocation; therefore, they need to wait until UE 25 performs its allocation. Finally, once both UEs allocate their respective slots, trigger time for UEs 5, 7, and 20 occurs, following the respective sequential order. A UE will not await the allocations of its higher priority ones indefinitely; therefore, the *resource selection delay*
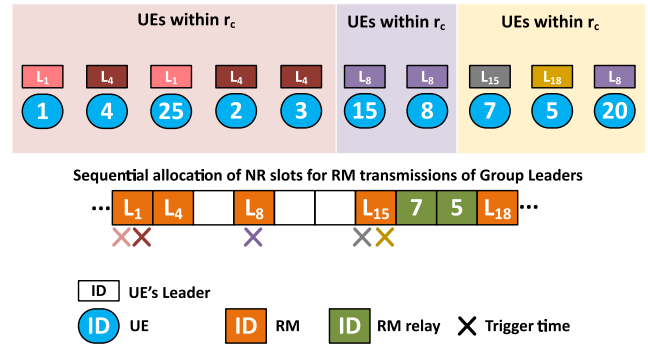
parameter is included to start the slot(s) selection when its value reaches zero. Additionally, two scenarios may happen if a user equipment (UE) changes its r_c (e.g., UE5 moves closer to UEs 15 and 8). First, UEs 15 and 8 already made their resource selection and shared it with all UEs within r_e, meaning that UE 5 is aware of it and can proceed to select its resources and send its RM. The second scenario contemplates that UEs are within a resource re-selection phase. Then, UE 5 adds to the sequence of UEs 8 and 15, and it will be the first of the three to allocate resources and send the RM.

B. GROUP SCHEDULING SCHEME

Unlike device sequential, group scheduling scheme builds on forming a group of UEs led by a chosen leader (i.e., group leader) who collects sensing results and simultaneously allocates slots for all group members. The group leader selection follows the evaluation of two steps: (a) determining which UE, within r_e, has the most UEs within its r_c, and (b) determine which UE has the lowest unique ID in case several UEs within r_e have the same value at (a). A group leader may also need to coordinate with other leaders present in its r_e or group members collaborating with UEs belonging to other groups. Group leader coordination follows a similar approach as the device sequential scheme by prioritizing leaders resource allocation based on first its trigger time and second its unique ID. After inter-leaders cooperation occurs, each group leader performs the resource allocation for its group members at their respective trigger times. Doing so requires two conditions. The first is group members sharing the number of slots they need, the results of the sensing phase, and the trigger time with their respective leaders well in advance. The second includes group leaders receiving resource allocation from higher priority leaders within its r_e. In our example shown in Fig. 5 UEs 1, 4, 25, 2, and 3 share the same r_c and trigger time (pink and orange crosses) but do not have selected the same group leaders (e.g., not necessarily share the same r_e). UEs 1 and 25 have L_1 leader who has higher priority than UEs 4, 2, and 3 denoted as leader L_4. Hence, leader L_1 performs resource allocation at the trigger time followed by leader L_4 in the next slot. Leaders L_{15} and L_{18} need assistance from their group members to allocate resources. In this case, UE 7

TABLE 1. Number of control signaling messages (Num. Messages) to achieve cooperative resource allocation in NR SL mode 2, device sequential and group scheduling.

RA Scheme	Num. Messages
Mode 2 IUC scheme 1 unicast request	n(2n-2)
Mode 2 IUC scheme 1 broadcast request	n^2
Device sequential	n
Group scheduling	1

FIGURE 6. NR slot with feedback capability used to perform HARQ and LAAG techniques when there is a data failure reception in a data period.

notifies UE 5 its received RM from L_{15} to be forwarded to L_{18} for its resource allocation.

It could occur that in all schemes, DMs experiment half-duplex with data messages (in all schemes), or UEs do not receive RMs coming from either high priority UEs or group leaders (cooperative schemes). To solve these issues, in [18] we introduced three techniques named as *non-overlappping*, *piggybacking*, and *RM re-transmissions*. *Non-overlapping* makes use of the sensing phase such that UEs avoid transmitting DMs in slots where an SPS transmission occurred to prevent potential half-duplex problems. *Piggybacking* refers to repeating the information received in RMs to append it into its RM. In the group scheduling scheme, it may happen that one or several group members were unable to receive the RMs coming from their leader. *RM re-transmissions* allows group members receive them by randomly re-transmitting a new RM in case a group member sends a negative acknowledgement (NACK).

Both device sequential and group scheduling resource allocation schemes represent a beneficial alternative to IUC, since they provide a considerable reduction of control signaling, which directly impacts the schemes' performance. For example, in a group consisting of *n* UEs, located within their respective critical cooperation range r_c, we determine the number of control signal messages required for mode 2 IUC scheme 1 and the cooperative schemes. 3GPP established unicast IUC request for mode 2 [36]. We named it as Mode 2 IUC scheme 1 unicast request. With the purpose of giving a fair degree of comparison, we assumed that mode 2 IUC is capable to broadcast IUC request. The number of control signal messages required for mode 2 IUC scheme 1 and the cooperative schemes is presented in Table 1.

IV. ENHANCEMENT TECHNIQUES FOR COOPERATIVE SCHEMES

HARQ and link adaptation techniques have been part of previous 3GPP releases and have evolved within time. Following, we present how HARQ has been adapted to mode 2 due to the network's absence, and our assumptions and procedure link adaptation follows by allocating additional resource(s) in our named link adaptation by aggregation LAAG technique.

A. HYBRID AUTOMATIC REPETITION REQUEST (HARQ)

HARQ builds on adding redundant information or performing more transmissions of the same data to increase communication r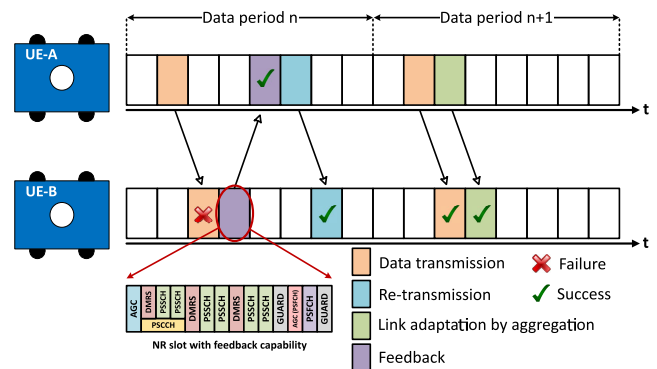eliability [37]. Our approach contemplates transmitting the same data repeatedly until it is successfully decoded at the receiver or the data period of 10 ms ends. Therefore, it is necessary to answer the following question: when should the first transmission be performed after the beginning of the data period? If it is done as early as possible, there will be enough time for additional re-transmissions at the cost of over occupying some portions of the data period of each UE when the swarm size increases. Additionally, they may be prone to perform more re-transmissions, expanding the resource occupancy, and hence, there might be higher interference or half-duplex problems. Our assumption contemplates a window of 30% of the data period (3.33 ms) for the first transmission while the remaining time is assigned for possible re-transmissions.

In 3GPP release 16, the mode 2's NR slot configuration to support HARQ was introduced [15]. It consists of reserving one of the fourteen OFDM symbols to the physical sidelink feedback channel (PSFCH), as shown in the zoomed slot structure in Fig. 6. The slot's structure periodicity is determined by the higher layer parameter *sl-PSFCH-Period-r16* defined in [38]. It is set to one of four possible values 0, 1, 2, and 4 that correspond to feedback disabled, feedback in all NR slots, every second NR slot, and every fourth NR slot, respectively. We have chosen the value of 1 to this parameter to allow all NR slots to be capable to transmit the PSFCH.

The PSFCH serves to make the transmitter notice the unsuccessful data reception by receiving an acknowledgement (ACK) or negative acknowledgment (NACK). This information is included in the 2nd stage SCI carried by the physical sidelink shared channel (PSSCH). Our approach considers the PSFCH carrying a NACK. The example shown in Fig. 6 presents how a data transmission coming from UE-A is not received by UE-B (orange slot with a red cross). UE-B sends a NACK in the PSFCH to make UE-A aware of the failure (purple slot). Once UE-A notices the failure, it proceeds to re-transmit data (blue slot), successfully received. If a data failure reception occurs again, the procedure repeats while there is still time remaining in the data period.

At the receiver, each re-transmission is combined with previous transmissions by adopting soft combining. It uses
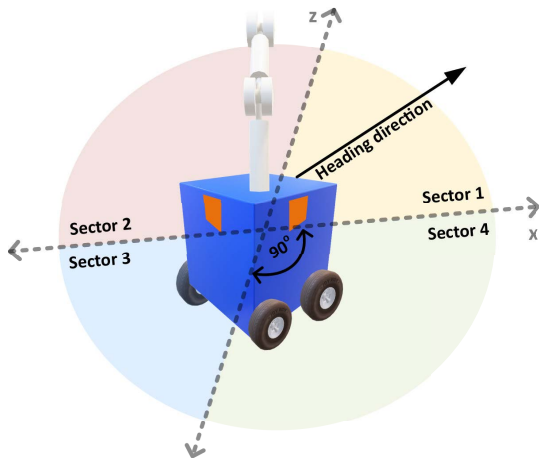
FIGURE 7. Directional antennas placed on each of the robot's chassis faces and the sectors correspondence according to the heading direction.

FIGURE 8. Transmitter and/or receiver antenna selection based on DM's reception and angle calculation of neighbors located within r_c. Each patch has its approx. radiation pattern.

chase combining [39] to obtain the resulting SINR of each re-transmission.

B. LINK ADAPTATION BY AGGREGATION (LAAG)

While HARQ focuses on making a failed data transmission successful, LAAG targets increasing the robustness of following data transmissions by allocating additional slot(s). It is done by using the feedback procedure HARQ has. Once a transmitter UE fails one transmission within the SPS period, it receives the first NACK from the receiver in the PSFCH, as detailed in Section IV-A. This NACK serves as a trigger of a UE's autonomous resource selection (i.e., no cooperation involved) that lasts until the end of the SPS period. The resource selection is random and allows the reduction of the modulation and coding scheme (MCS) index of subsequent transmissions to increase its robustness. In our example shown in Fig. 6 UE-A performs a HARQ re-transmission at data period n where it selects an additional slot for its transmission at data period $n + 1$. Given that an additional slot was allocated, the MCS index was reduced, making the next transmission successful and hence, avoiding a possible new HARQ re-transmission.

The two previous techniques support mode 2 and cooperative schemes to prevent and recover from data transmission failures by re-transmitting the same information in other NR slot(s) or by allocating additional slot(s) to reduce the previous selected MCS. None of them considers techniques to boost the SINR to avoid re-transmissions or additional slot(s) allocation. In the following, we explore it by recapitulating our design for antenna directivity and beam selection.

C. ANTENNA DIRECTIVITY AND BEAM SELECTION

A UE equipped with an isotropic antenna radiates its signal in the whole 360-degree range, making it possible to reach others that are not within its r_c. Therefore, the cause of interference becomes more critical as the swarm size increases.
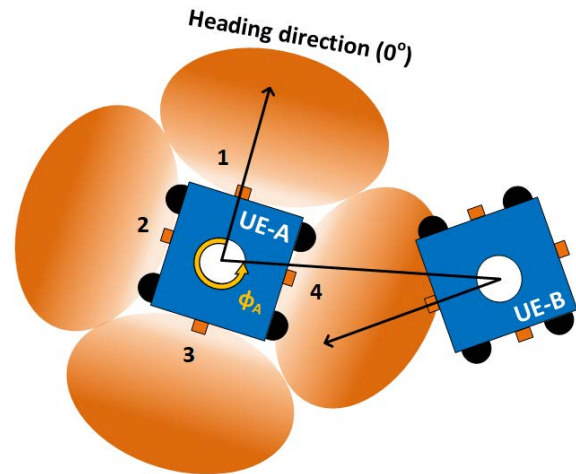
In [31] we adopted the configuration of a type 2 vehicle specified in [40] to limit UE's signal radiation range to 90 degrees. It equips each robot with four directional antennas, each placed on one face of the robot's chassis. Each antenna creates a beam that should cover a specific 90-degree azimuth sector, denoted as sectors 1, 2, 3, or 4. The robot's face that follows the heading direction corresponds to sector 1 followed by the others in an anti-clockwise ascendant order. Fig. 7 shows the robot's chassis, the directional antennas (orange squares) placed on them, and the sector that corresponds to each one. Sector 1 is identified with yellow, while sectors 2, 3, and 4 are red, blue, and green, respectively.

As stated before, each directional antenna forms a beam with gain $g(\theta, \phi)$ to cover its respective sector. UEs select one or several beams by considering the position of others located within its critical cooperation range r_c to transmit, receive or transmit and receive data. To do so, UEs leverage the context information [41] (e.g., coordinates, speed and heading direction) instead of relying on a power-based beam selection [42]. The context information is shared by simultaneously broadcasting/listening to DMs in all UE's beams. This allows them to estimate others current and near-future positions to determine those who are entering their respective critical cooperation range r_c, becoming target UEs for data transmissions. It is assumed that UEs have enough time to proceed with beam switching since DM's periodicity provides sufficient discovery probability [18]. The UEs' estimation lets the transmitter UE select the beam presenting the highest gain in the relative horizontal orientation (i.e., angle ϕ_{ID}) towards the target receiver. This process repeats, in the same fashion, for beam selection for data reception. In our example in Fig. 8, transmitter UE-A faces receiver UE-B at an azimuth value of ϕ_A. It corresponds to being in the direction of beam number four, being the one selected for data transmission. The beam color, analogous to the beam's gain, degrades as the angle deviates from the

patch's boresight (i.e., the direction in which the patch has its maximum gain), as shown in Fig. 9.

V. SYSTEM LEVEL EVALUATION

As introduced in Section II, our use case scenario centers on decentralized communications for a swarm of mobile robots in an industrial factory. We assumed an indoor factory facility of dimensions 120 by 50 meters, the same specified by 3GPP in [43]. Data transmissions occur when robots get into a critical cooperation range r_c of 5 meters to get a collective perception of the environment (i.e., awareness of the presence of other robots and obstacles). The communication requirements for this scenario go beyond the ones currently in vehicle to anything (V2X) as envisioned in [16] contemplating a 10 Mbps throughput, 10 ms of latency, and 99.99% reliability.

A. SYNCHRONIZATION

Since our baseline scheme is mode 2, we assume that the robots in the swarm acquire their time and frequency synchronization from the 5G NR SL synchronization procedure [44]. Note that for NR sidelink, the synchronization is not established between two-peer UEs but instead is acquired by these peer UEs from a common source. NR SL has two primary sources for synchronization: a global navigation satellite system (GNSS) and a gNB or eNB (referred to as gNB/eNB). In addition, a UE can use a SyncRef UE or its own internal clock as its synchronization reference. Finally, note that the synchronization procedure is separate from the communication procedure.

B. CHANNEL MODEL

The wireless channel model follows the 3GPP indoor factory path loss model [43], assuming that all links are non-line-of-sight (NLOS) and single input single output (SISO) as presented in equation (1)

$$L_{dB} = \beta + \alpha \times 10 \log_{10}(d) + \psi \times 10 \log_{10}(f_c), \quad (1)$$

where α is the NLOS path loss exponent, β is the reference offset, d is the distance between transceivers, ψ is the frequency factor, and f_c is the carrier frequency. The estimated channel gain in dB is given by

$$H_{g,dB} = -L_{dB} - X_{dB}, \quad (2)$$

where X_{dB} is the correlated shadowing obtained from a Gaussian random field [45]. The covariance function is defined by the shadowing standard deviation (σ) of 5.7 dB and an exponential decaying correlation with a de-correlation distance (δ) of 20 meters. Small-scale fading due to multipath has not been explicitly modelled, but included in the link layer model [18]. The correspondent linear gain is

$$h_g = 10^{\frac{H_{g,dB}}{10}}. \quad (3)$$

C. DIRECTIONAL ANTENNA MODEL

The function $A_{dB}(\theta, \phi)$ expresses the power distribution of the directional antenna in the horizontal and vertical planes
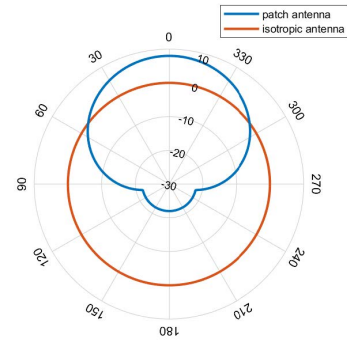

FIGURE 9. 2D radiation pattern of an isotropic antenna and 3GPP directional antenna for 360° azimuth angles represented over the $\theta = 90^o$ plane.

by making use of spherical coordinates (θ, ϕ) [43]. The horizontal and vertical radiation patterns are denoted as $A_{H,dB}(\phi)$ and $A_{V,dB}(\theta)$, respectively. $A_{H,dB}(\phi)$ is given by

$$A_{H,dB}(\phi) = -\min\left\{12\left(\frac{\phi}{\phi_{3dB}}\right)^2, A_{max}\right\}, \quad (4)$$

where ϕ_{3dB} is the horizontal half power beam width (HPBW) of the directional antenna, A_{max} is the front to back ratio, which is the ratio of magnitude between the main lobe at 0° and the back lobe at 180° of a radiation pattern [46], [47], and the value of ϕ can be between $[-180^o, 180^o]$. Similarly, $A_{V,dB}(\theta)$ is defined as

$$A_{V,dB}(\theta) = -\min\left\{12\left(\frac{\theta - 90^o}{\theta_{3dB}}\right)^2, SLA_V\right\}, \quad (5)$$

where θ_{3dB} is the vertical HPBW of the directonal antenna and SLA_V is the vertical direction side-lobe attenuation, and the value of θ can be between $[0^o, 180^o]$.

Finally, the directional antenna's 3D radiation power pattern is computed as

$$A_{dB}(\theta, \phi) = G_{max} - \min\left\{-\left(A_{V,dB}(\theta) + A_{H,dB}(\phi)\right), A_{max}\right\}, \quad (6)$$

where G_{max} is the maximum directive gain. The correspondent linear gain is

$$g(\theta, \phi) = 10^{\frac{A_{dB}(\theta, \phi)}{10}}. \quad (7)$$

We use a value of 65°, adopted by 3GPP in [43], for ϕ_{3dB} and θ_{3dB} since it gives the highest possible gain to the directional antenna [31]. Additionally, we assume all robots have the same height, meaning directional antennas placed on their chassis are facing each other at the same level. Therefore, the vertical angle θ has a fixed value of 90 degrees, and $g(\theta, \phi)$ simplifies to $g(\phi)$ where angle ϕ changes based on the transmitter and/or receiver position.

The directional antennas parameter values are presented in Table 2 while its radiation pattern, juxtaposed with an isotropic one, is shown in Fig. 9.

D. SIGNAL-TO-NOISE-PLUS-INTERFERENCE RATIO

Each robot requires a 100 Kbit data transmission for each 10 ms to achieve the target 10 Mbps. It would require it to allocate more than one NR slot. The number of slots, K, required by each robot is obtained when choosing an appropriate MCS, from [15, Table 5.1.3.1-2], with an expected block error rate (BLER) of 0.01%. Each of these K allocated slots will experience an SINR (γ_k) value depending on the number of robots in the swarm and the chosen resource allocation scheme. Equation (8) presents the expression that fits all beam selection configurations where transmitter and receiver beam selection are enabled. We adopted the maximum ratio combining (MRC) technique [48] that adds all the S received signals as follows,

$$\gamma_k = \sum_{z=1}^{S} \left(\frac{\frac{p_{tx}}{N} \times \left(\sum_{j=1}^{N} \sqrt{g(\phi_{t_j})} \right)^2 \times h_g \times g(\phi_{r_z})}{\sum_{i=1}^{I}(\frac{p_{tx_i}}{N_i} \times \left(\sum_{j=1}^{N_i} \sqrt{g(\phi_{t_{i_j}})} \right)^2 \times h_{g_i}) + n} \right), \tag{8}$$

where the transmission power, gain at each active transmitter beam and the channel gain correspond to $p_{tx}, g(\phi_{t_j})$ and h_g, respectively. The corresponding values for the ith UE interferer(s) are $(p_{tx_i}, g(\phi_{t_{i_j}}), h_{g_i})$. At each active receiver, the beam gain is denoted as $g(\phi_{r_z})$. Finally, the additive white gaussian noise (AWGN) is represented by n. All previous introduced values are linear.

In transmitter beam selection, UEs can activate up to four beams ($N \in \{1, 2, 3, 4\}$). Given that, we require UEs to radiate the same transmission power regardless of the number of active beams. To achieve it, we assume a coherent combination of transmissions coming from each beam (voltage summation) and a proportional transmission power reduction each time more than one beam activates (i.e., $\frac{p_{tx}}{N}$, $\frac{p_{tx_i}}{N_i}$ in equation (8)). There might be an exceptional case where one receiver UE is located between two beams. Then the two beams will be active, ending up having an effective radiated power equivalent to twice the transmission power of each of the beams at that specific angle (ϕ). The other cases approximate the assumed proportional reduction, corresponding to the desired beam contributing significant power. Similar to transmitter beam selection, receiver beam selection allows UE to activate up to four beams ($N \in \{1, 2, 3, 4\}$). The main difference lies in this configuration is that UEs are more likely to only activate one beam. Activating more beams makes the receiver more sensitive to half-duplex problems (i.e., data transmissions within UE's r_c colliding in reception). The exemption to this case is where a receiver UE needs to receive data from transmitters that do not share the same r_c.

E. EFFECTIVE SINR

We use each of these γ_k values, measured on the most recent transmission, to determine the effective SINR (γ_{MIC}) by adopting the mean instantaneous capacity (MIC) method,

explained in [49], as follows,

$$\gamma_{MIC} = 2^{\frac{1}{K} \sum_{k=1}^{K} log_2(1+\gamma_k)} - 1, \tag{9}$$

where K is the number of allocated slots, and γ_k is the SINR value at the kth slot. The mapping of effective SINR (γ_{MIC}) to BLER, given the chosen MCS, is done by using a set of BLER curves that were obtained through separate link-level simulations that include all physical layer processing according to 5G NR [50].

In presence of half-duplex (e.g., with DMs, RMs or other data transmissions) in one k^{th} allocated slot, the spectral efficiency ($log_2(1 + \gamma_k)$), equation (9), in that slot will be zero [bps/Hz]. This data loss will impact to a greater or lesser degree the γ_{MIC}, equation (9), value depending on the number of slots experimenting half-duplex since it has to be high enough for the selected MCS to have a successful reception. In case all K allocated slots experience half-duplex, for sure, the receiver will not be able to decode the data message.

F. HARQ

At the receiver, each re-transmission is combined with previous transmissions by using chase combining [39] to obtain the resulting SINR (γ_{CC}) of the ith re-transmission as follows,

$$\gamma_{CC} = \sum_{i=0}^{RT} \gamma_i \times \eta^{RT}, \tag{10}$$

where RT is the number of re-transmissions, η is the combining efficiency factor and γ_i is the SINR of the ith (re-) transmission, being the first transmission when $i = 0$. We assume a $\eta = 1$ for our implementation.

G. NR PARAMETERS

When looking at the 5G NR parameters, we select numerology 2, giving a slot duration of $d_s = 0.25$ ms. For the control channel (where DMs and RMs are transmitted), we choose the value of 7.2 MHz since it is the smallest configurable sidelink sub-channel which consists of twelve sub-carriers. Additionally, we select the lowest MCS having a modulation order of 2 and a code rate of $\frac{120}{1024}$, leaving 196 bits for usage. On the other hand, the data channel bandwidth is set to 100 MHz. In contrast to the control channel, the MCS is dynamically adapted at the time of allocation [18]. The link-level model does not differentiate between data and control signal transmissions making the latter's performance somewhat optimistic given the considerable difference in bandwidth (i.e., 100 MHz vs. 7.2 Mhz) [18]. All simulation parameters are listed in Table 2.

H. CONFIGURATIONS

Our goal is to present the increment of the number of UEs fulfilling the requirements of 10 Mbps throughput, 10 ms latency, and 99.99% reliability by progressively enabling the different enhancing techniques for the three resource allocation schemes (mode 2, device sequential, and

TABLE 2. Simulation parameters.

Parameter	Value/range
Carrier frequency, f_c	3.5 GHz
Swarm size (N_r number of UEs)	[20, 50, 70, 90]
Critical cooperation range, r_c	5 m
Extended Cooperation range, r_e	25 m
Facility dimensions	120×50 m^2 [43]
Transmission power, P_{tx}	0 dBm
Data channel bandwidth	100 MHz
Control channel bandwidth	7.2 MHz
Resource selection delay	1.25 ms
NR slot duration	250 μs
Thermal noise power spectral density	-174 dBm/Hz
Receiver noise figure	9 dB
Interference	Independent intra-system
UE speed	1 m/s
Mobility model	Random waypoint (RWP)
Pathloss model	InF-SL [43]
Propagation condition	Non line of sight
De-correlation distance δ	20 m [45]
Shadowing standard deviation σ	5.7 dB [45]
Discovery message periodicity	100 ms
Data message periodicity,	10 ms
Data message size,	100 kb
Data message latency requirement,	10 ms
sl-PSFCH-Period-r16	1 ms [38]
Scheduled Tx slots window	3.33 ms [25]
RTx slots window	6.67 ms [25]
Number of antenna elements	4
HPBW (θ_{3dB})	65° [43]
SLA_V	30 dB
A_{max}	30 dB
G_{max}	8 dBi
Simulation time	1000 s

group scheduling). Our evaluations consider three configurations applied for the three schemes, which are the following:

1) **Enhanced error-prone signaling** in which non-overlapping and piggybacking techniques (explained in Section I) are enabled to avoid half-duplex between DMs and data, and RMs and data.

2) **HARQ LAAG** in which in addition to 1) hybrid automatic repeat request (HARQ) and link adaptation by aggregation (LAAG) techniques are enabled to provide time diversity to overcome data failure receptions.

3) **Tx & Rx beam selection** in which in addition to 2) transmitter and receiver beam selection are simultaneously enabled since it provides the best performance to mode 2 in [31]. It increases the effective SINR (γ_{MIC}) and avoids data failure receptions despite the presence of half-duplex in some data segments.

VI. SIMULATION RESULTS

The performance of each of the resource allocation schemes depends on how the resource allocation procedure avoids the presence of half-duplex problems and manages interference. To evaluate it, we selected three KPIs to perform **five studies** presented in Table 3. Each study adopts one or several of the configurations presented in Section V-H.

Failure Probability (f_p): defined as the probability of not receiving a transmitted 100 kb data message within 10 ms latency. It is directly linked with reliability as presented

TABLE 3. Performed studies.

Study	KPI	Configuration
A.Error-prone signaling	average failure rate	1
B. HARQ & LAAG	average failure rate	2
C. Beam selection	average failure rate	3
D. Reliability	failure probability	1, 2, 3
E. Latency	PIR	1, 2, 3

in equation (11)

$$f_p = 1 - r_p \tag{11}$$

where r_p is the reliability. A reliability of 99.99% corresponds to 10^{-4} failure probability.

Average Failure Rate Per NR Slot (fr_s): defined as the average rate of NR slots experiencing half-duplex or interference that lead up into unsuccessful reception. fr_s is given by

$$fr_s = \frac{\sum N_f}{N_r \times T} \tag{12}$$

where N_f is the per UE number of slots experiencing failures, N_r is the swarm size, and T is the number of NR slots in the simulation time. We present it in detail by including the portion that corresponds to each kind of failure. For half-duplex, it could appear as data and discovery messages (data-DMs), data and resource selection messages (data-RMs), or between data (data-data). Interference could appear as inner, outer or mixed. Inner interference refers to harmful transmissions originating from UEs located within r_c, while if they originate within r_e, it corresponds to outer interference. Mixed interference indicates the simultaneous presence of the previous two. We link these results to the mean resource occupancy per NR slot (i.e., the average number of UEs occupying the same NR slot for data transmission).

Packet Inter-Reception (PIR): defined by 3GPP in [40]. It indicates the time between successive packet receptions and is an important metric for applications requiring regular updates.

For studies A, B, and C, we use average failure rate as the KPI to give a fair comparison of the benefits or disadvantages each scheme or technique has in performance; what is of interest here are the lower percentiles. For studies D and E, we use the failure probability and PIR KPIs, respectively, to compare the performance of mode 2 with the cooperative schemes in the three configurations.

We adopted a confidence interval of 95% to our simulations, similar to [51]. In our approach, we have been running simulations progressively, in each step estimating the 95% confidence interval for the obtained results based on the non-parametric bootstrap method [52]. In case the estimated interval exceeded the desired accuracy target, simulations continued to include more (random) samples until enough samples were collected. The simulation time (i.e., the sum of all simulation times in the different simulations) provided 95% of values with a zero standard deviation of the mean PIR distribution at the 99.99 percentile.
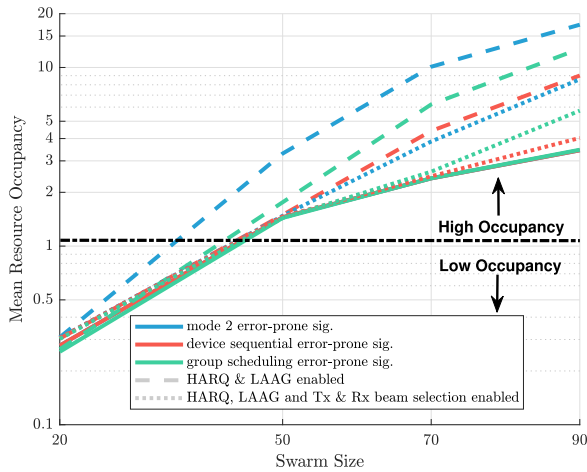
FIGURE 10. Mean resource occupancy for swarm sizes of 20, 50, 70 and 90 UEs. Mean occupancy below one is considered as low.
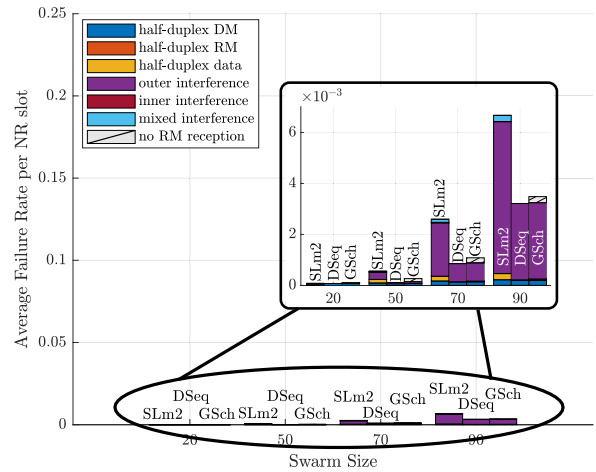

FIGURE 11. Average failure rate per NR slot at configuration 1 for the three resource allocation schemes: mode 2 (baseline), device sequential, and group scheduling, for four swarm sizes.

A. AVERAGE FAILURE RATE WITHOUT ENHANCEMENTS

Fig. 11 shows the average failure rate for the error-prone signaling configuration. The main cause of failure lies in outer interference, which significantly increases with the swarm size. Mode 2 handles it worse due to its random resource selection which also causes the presence of half-duplex data transmissions, as expected. The cooperative schemes avoid half-duplex data and substantially reduce outer interference since the resource selection control signaling makes UEs select as orthogonal slots as possible; otherwise, the ones where interference is the lowest. Since data transmission failures cannot be recovered in this configuration, the three schemes have the same average resource occupancy per NR slot for all swarm sizes as Fig. 10. Then, the difference lies in how each scheme handles resource allocation.

Additionally, even though a non-overlapping technique (described in Section I) was applied, there is the presence of some half-duplex of data and discovery messages (DMs), navy blue bar portions. The growth of the swarm size makes UEs increment the SINR threshold within the sensing procedure to increment the set of candidate slots, making the mean resource occupancy reach values above 1. Consequently, the random selection of slots for DM transmissions might overlap a few data transmissions. The group scheduling scheme presents a unique behavior caused by the dependency on a group leader. There are cases where group members do not receive resource selection messages (RMs). The RM re-transmission technique considerably diminishes this issue, but a few RMs are still not received. As a result, a few UEs are deprived of any data transmission, making it impossible to recover that data by using HARQ, LAAG, or beam selection techniques. For that reason, we have added a rebel-sub mode to the UEs, which does not deteriorate the general performance of the group scheduling scheme.

1) REBEL SUB-MODE

The group leader UE sends an RM to its group members containing their allocated slots at some point close to the
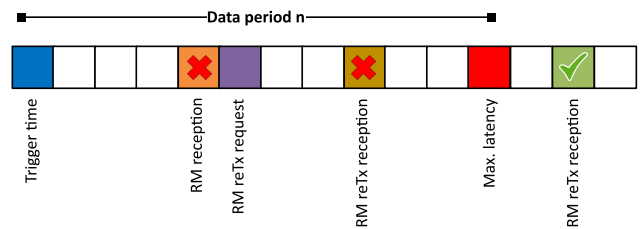
FIGURE 12. RM re-transmissions problem that ends up in having a data transmission failure that neither HARQ nor LAAG can recover.

trigger time, depending on if the leader must follow a sequential allocation, edge cases, etc., as explained in Section III-B. It shortens the time group members have to perform data transmissions within the data period started at the trigger time. If the RM reception fails as the orange slot in Fig. 12, the group member sends an RM re-transmission request to its leader, which is also prone to a failed reception at the leader side. If it is successfully received, the procedure repeats until the group member successfully receives it. In our example in Fig. 12, the leader performs two RM re-transmissions to reach the group member. However, unfortunately, it happens after the maximum latency allowed in the data period n. Hence, there is no data transmission, and it is considered a failure due to no RM reception. On the other hand, if the leader doesn't receive the RM re-transmission request, the group member UE will continue sending these requests until it gets one successfully. Again, it can overpass the maximum latency allowed in the data period, and it is considered a failure due to no RM reception.

We enhanced our group scheduling scheme by not relying on the RM re-transmissions as before to solve this issue. Instead, a group member UE, who did not receive their respective RM, rebels against its leader. It proceeds to follow the group scheduling considering itself as the unique UE for the group. Therefore, it contemplates itself as a leader

FIGURE 13. Average failure rate per NR slot at configuration 1 after the incorporation of rebel sub-mode for the three resource allocation schemes: mode 2 (baseline), device sequential, and group scheduling, for four swarm sizes.

FIGURE 15. Average failure rate per NR slot at configuration 3 for the three resource allocation schemes: mode 2 (baseline), device sequential, and group scheduling, for four swarm sizes.
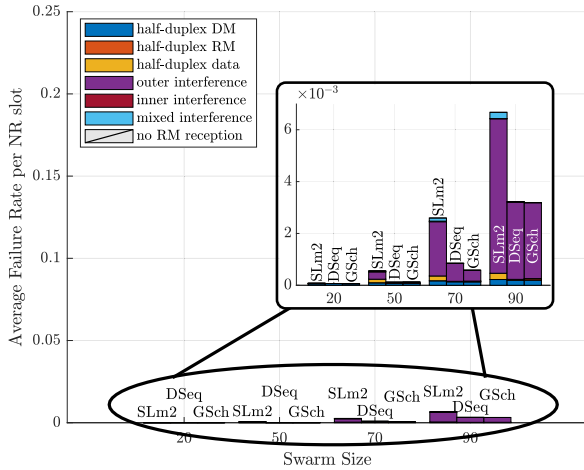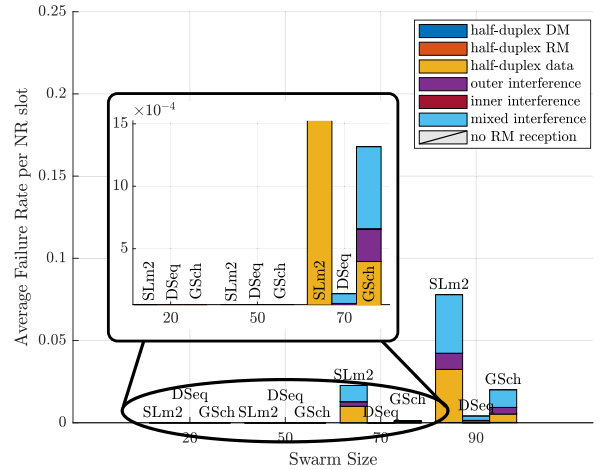

FIGURE 14. Average failure rate per NR slot at configuration 2 for the three resource allocation schemes: mode 2 (baseline), device sequential, and group scheduling, for four swarm sizes.
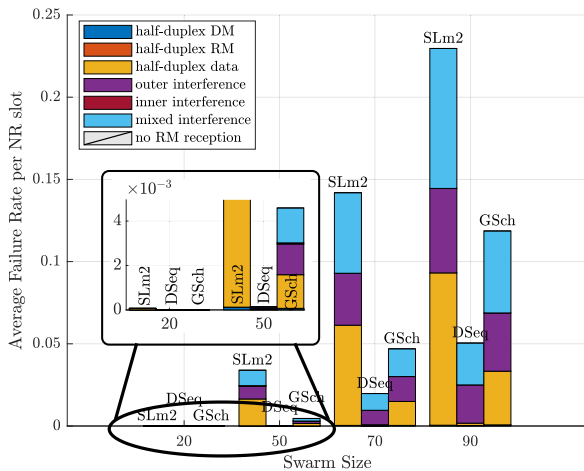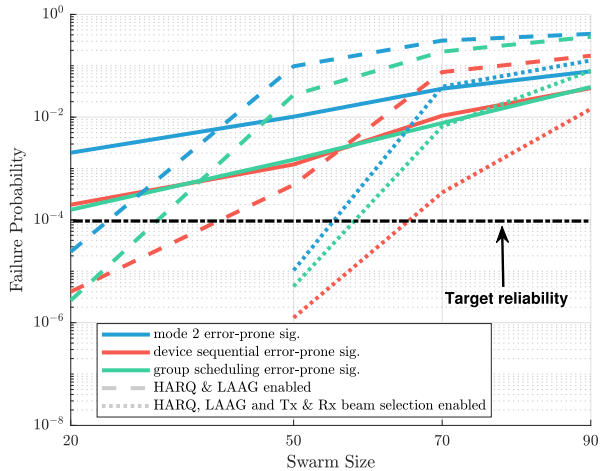

FIGURE 16. Failure probability achieved at three configurations for the four swarm sizes. The 10^{-4} requirement is indicated by the dashed black line.

and group member simultaneously. The benefit is that the UE takes advantage of the information obtained in mode 2's sensing procedure, the one obtained in the DMs and the group scheduling scheme benefits. It is seen in Fig. 13 that all bar portions corresponding to no RM receptions are eliminated due to rebel sub-mode. Therefore, the certainty of having data failures due to the lack of leader's resource allocation disappears.

B. AVERAGE FAILURE RATE WITH HARQ & LAAG

When enabling HARQ and LAAG, configuration 2, it is noticeable the increment of mode 2's mean resource occupancy in comparison to device sequential and group scheduling schemes in Fig. 10 (dashed lines). Device sequential and group scheduling have the same mean resource occupancy until the swarm size reaches a value of 50 UEs. Beyond that swarm size, device sequential is the one experiencing

the lowest. Mode 2's random selection of slots makes UEs prone to need more re-transmissions and additional slot(s) allocation. Fig. 14 shows the average failure rate for this configuration. Mode 2 presents the highest value and the higher presence of data half-duplex (yellow bar portions). Cooperative schemes keep their average failure rate significantly lower than mode 2, even though they present a lower amount of data half-duplex in larger swarms where UEs tend to be closer. In the case of group scheduling, even though UEs share the same r_c, they could have different group leaders who might not be aware of each other's resource allocation, ending up in half-duplex problems. In device sequential, these tiny cases appear when large sequences of UEs appear, exhausting the resource selection delay and making it feasible for UEs to select the same slot. Interference-wise, it is more likely that data failures are due to mixed interference than outer interference in mode 2. At the same time, device sequential
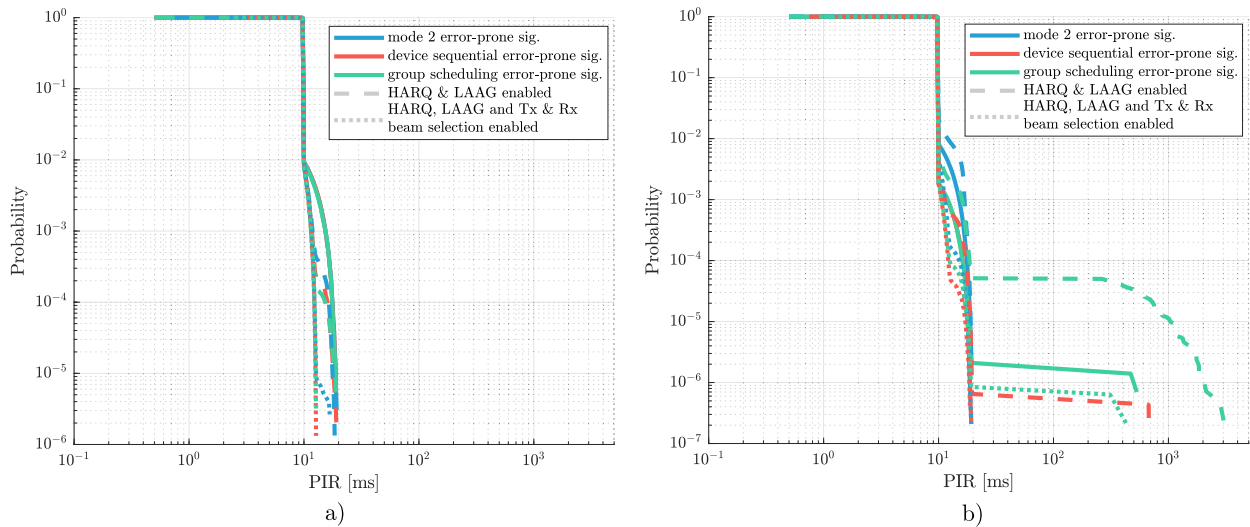
FIGURE 17. Packet inter reception (PIR) complementary CDF at swarm sizes of 20 UEs (a) and 50 UEs (b) for the three simulation configurations.

and group scheduling, both kinds of interference, keep the same proportion.

C. AVERAGE FAILURE RATE WITH BEAM SELECTION

A vast proportion of all kinds of interference and a considerable one of data half-duplex encountered in configuration 2 are reduced when enabling transmitting and receiving beam selection to all the schemes in Fig. 15. It is because the gain of a beam decreases as interferers get far from the boresight, making UEs use fewer slots for HARQ and LAAG since UEs boost the SINR at the transmitter and receiver sides. Then, a substantial reduction of the bar portions corresponding to half-duplex and interference is noticeable compared to Fig. 14. Even though beam selection gives the best performance to all schemes, mode 2 still requires more re-transmissions than cooperative schemes translating it to a higher mean resource occupancy and average failure rate of the three, confirming the benefit of using cooperative schemes.

D. FAILURE PROBABILITY AND SWARM's DENSITY

The average failure rate per NR slot and mean resource occupancy gave us an impression of how the resource allocation scheme makes usage of NR slots in the three configurations. The failure probability and swarms' density indicate how many UEs fulfill the stringent communication requirements. Fig. 16 presents both for all configurations and swarm sizes. Cooperative schemes support a larger swarm size than mode 2 in all configurations. It is clearly seen that group scheduling is not considerably distant from mode 2's performance. The findings of this study suggest the incorporation of the rebel sub-mode in the group scheduling scheme, which makes it less *"cooperative"* when a UE becomes leader and group member itself. Even though these cases might happen, the overall performance of group scheduling allows it to

increment a bit the swarm's size. A considerable increase is seen with the device sequential scheme, where it reaches approximately 20% more UEs than mode 2 when both enable all techniques. It confirms that cooperative communication with autonomy represents a better solution for this setup. Forming groups led by some UEs degrades the performance as the swarm's size increases because UEs will belong to different groups and need to transmit data between them, requiring group leaders to exchange RMs. However, it also might happen to device sequential scheme. The difference is that it only happens with the resource selection of one UE, so the impact of an unacknowledged RM will be by far less than a group of RMs in the group scheduling scheme. Therefore, we can conclude that cooperation and UEs' independence are two important factors when designing decentralized cooperative resource allocation schemes that fulfill stringent requirements.

E. IMPACT OF THE SCHEMES' NUMBER OF CONTROL SIGNALING MESSAGES

Our simulator does not have IUC functionality. However, the analysis of the number of control signaling messages required by mode 2 (unicast and broadcast IUC request) and our proposed cooperative schemes would be beneficial in drawing some conclusions. In Section III, Table 1 showed the number of control signal messages mode 2 IUC and our proposed schemes require to perform cooperative resource allocation. Mode 2 IUC requires a more significant amount of control signaling messages than device sequential and group scheduling, even though IUC request was assumed to be broadcast. Therefore, it is prone to experience higher interference since the separate resource pool might be more occupied. Consequently, data transmissions will occur in the same slots where other UEs (our of r_c) transmit IUC requests. Device sequential and group scheduling are promising options for

this problem since they achieve the same level of cooperation as mode 2 IUC by using significantly fewer control signaling messages. Additionally, they represent a promising solution when considering other performance aspects, such as UEs' energy consumption.

F. PACKET INTER-RECEPTION (PIR)

Fig. 17 (a) and (b) show the complementary CDF of the PIR for respectively, 20 and 50 UE swarm size simulations. We did not consider other swarm sizes since we wanted to present the PIR's behavior before and after reaching the maximum supported swarm size in all configurations. The fact that semi-persistent transmissions make possible successful receptions of a series of data messages resulting in a 10 ms PIR. PIR values under 10 ms, or between 10 ms and 20 ms, are due to the re-selection of SPS transmission. However, if they go beyond that value, it represents a data failure reception. The resource allocation scheme and configuration with the highest failure probability also experiences the longest PIR. At 20 UE swarm size, the PIRs exceed 10 ms with a probability less than 10^{-2}. All schemes with beam selection enabled keep the lowest PIR with a tiny difference that the cooperative ones maintain below a probability of 10^{-5}, which is impossible with mode 2. At 50 UE swarm size, the cooperative schemes are the ones experiencing PIRs greater than hundreds of milliseconds but for with probability below 10^{-4}. It is eliminated by the incorporation of beam selection for device sequential but remains for group scheduling for probability below 10^{-6}.

VII. CONCLUSION

The release 16 of 5G NR sidelink mode 2 decentralized resource allocation scheme didn't provide cooperative capabilities to avoid half-duplex problems. Current release 17 includes coordination capabilities; however, the need for numerous signaling messages to perform inter-UE coordination (IUC) and random resource allocation makes it challenging to fulfill the stringent requirements of 99.99% reliability, 10 Mbps throughput, and 10 ms latency. In comparison, it is clear that *device sequential* and *group scheduling* schemes are beneficial due to the considerable reduction of control signaling, directly outperforming mode 2.

The methodology of identifying the causes of the average failure rate per NR slot allowed us to identify the more representative ones to reduce them with the application of enhancement techniques. Three enhancement techniques, respectively, HARQ, LAAG, and beam selection, were introduced to address these problems and allow the increment of the supported swarm size. Although cooperative resource allocation schemes use signaling overhead, they provide an order of magnitude reduction in failure probability compared to mode 2.

HARQ and LAAG allow UEs to add redundancy and robustness by reducing the MCS of data transmissions. The side effect is the increment of the mean resource occupancy as the swarm size increases, producing more half-duplex

problems in the case of mode 2 and all kinds of interference for all schemes. Beam selection copes with many of these problems by using directional antennas to reduce the impact of undesired transmissions. Cooperative schemes, specifically device sequential scheme, give an additional 20% of swarm density compared to mode 2; however, interference and a few half-duplex problems become significant when increasing the swarm size.

Interesting topics to be explored in the future include the study of energy consumption together with the adaptive selection of cooperative resource allocation schemes when the swarm size changes dynamically. The study of power allocation would undoubtedly be beneficial to manage the interference when the swarm size overpasses seventy UEs and potentially increases the supported swarm size even further than that value. Finally, a study of the incorporation of network coding principles to our device sequential and group scheduling would allow exploring if additional coordination is required to get its benefits.

REFERENCES

[1] I. Rodriguez, R. S. Mogensen, A. Schjorring, M. Razzaghpour, R. Maldonado, G. Berardinelli, R. Adeogun, P. H. Christensen, P. Mogensen, O. Madsen, C. Moller, G. Pocovi, T. Kolding, C. Rosa, B. Jorgensen, and S. Barbera, "5G swarm production: Advanced industrial manufacturing concepts enabled by wireless automation," *IEEE Commun. Mag.*, vol. 59, no. 1, pp. 48–54, Jan. 2021. [Online]. Available: https://ieeexplore.ieee.org/document/9356516/

[2] Y. Tan and Z. Zheng, "Research advance in swarm robotics," *Defence Technol.*, vol. 9, no. 1, pp. 18–39, Mar. 2013.

[3] K.-C. Chen, S.-C. Lin, J.-H. Hsiao, C.-H. Liu, A. F. Molisch, and G. P. Fettweis, "Wireless networked multirobot systems in smart factories," *Proc. IEEE*, vol. 109, no. 4, pp. 468–494, Apr. 2021.

[4] W. Xia, J. Goh, C. A. Cortes, Y. Lu, and X. Xu, "Decentralized coordination of autonomous AGVs for flexible factory automation in the context of industry 4.0," in *Proc. IEEE 16th Int. Conf. Autom. Sci. Eng. (CASE)*, Hong Kong, Aug. 2020, pp. 488–493.

[5] R. Rey, M. Corzetto, J. A. Cobano, L. Merino, and F. Caballero, "Human–robot co-working system for warehouse automation," in *Proc. 24th IEEE Int. Conf. Emerg. Technol. Factory Autom. (ETFA)*, Sep. 2019, pp. 578–585.

[6] E. Lyczkowski, A. Wanjek, C. Sauer, and W. Kiess, "Wireless communication in industrial applications," in *Proc. 24th IEEE Int. Conf. Emerg. Technol. Factory Autom. (ETFA)*, Zaragoza, Spain, Sep. 2019, pp. 1392–1395.

[7] A. Varghese and D. Tandur, "Wireless requirements and challenges in industry 4.0," in *Proc. Int. Conf. Contemp. Comput. Informat. (IC3I)*, Nov. 2014, pp. 634–638.

[8] S. K. Rao and R. Prasad, "Impact of 5G technologies on industry 4.0," *Wireless Pers. Commun.*, vol. 100, no. 1, pp. 145–159, May 2018, doi: 10.1007/S11277-018-5615-7.

[9] J. Haxhibeqiri, E. A. Jarchlo, I. Moerman, and J. Hoebeke, "Flexible Wi-Fi communication among mobile robots in indoor industrial environments," *Mobile Inf. Syst.*, vol. 2018, Apr. 2018, Art. no. 3918302, doi: 10.1155/2018/3918302.

[10] I. O. Sanusi, K. M. Nasr, and K. Moessner, "Radio resource management approaches for reliable device-to-device (D2D) communication in wireless industrial applications," *IEEE Trans. Cognit. Commun. Netw.*, vol. 7, no. 3, pp. 905–916, Sep. 2021.

[11] D. Feng, L. Lu, Y. Yuan-Wu, G. Li, S. Li, and G. Feng, "Device-to-device communications in cellular networks," *IEEE Commun. Mag.*, vol. 52, no. 4, pp. 49–55, Apr. 2014.

[12] P. Pawar and A. Trivedi, "Device-to-device communication based IoT system: Benefits and challenges," *IETE Tech. Rev.*, vol. 36, no. 4, pp. 362–374, Jul. 2019, doi: 10.1080/02564602.2018.1476191.

[13] F. Wu, H. Zhang, B. Di, J. Wu, and L. Song, "Device-to-device communications underlaying cellular networks: To use unlicensed spectrum or not?" *IEEE Trans. Commun.*, vol. 67, no. 9, pp. 6598–6611, Sep. 2019.

[14] C. Chakraborty and J. J. C. P. Rodrigues, "A comprehensive review on device-to-device communication paradigm: Trends, challenges and applications," *Wireless Pers. Commun.*, vol. 114, pp. 185–207, Sep. 2020, doi: 10.1007/S11277-020-07358-3.

[15] *Physical Layer Procedures for Data*, 3GPP, document TR 38.214 V16.0.0, Dec. 2019.

[16] *Study on Enhancement of 3GPP Support for 5G V2X Services*, 3GPP, document TR 22.886 V16.2.0, Dec. 2018.

[17] S. Morejon, R. Bruun, T. Sørensen, N. Pratas, T. Madsen, J. Lianghai, and P. Mogensen, "Cooperative resource allocation for proximity communication in robotic swarms in an indoor factory (forthcoming)," in *Proc. IEEE Wireless Commun. and Netw. Conf.*, Nanjing, China, Mar. 2021, pp. 1–6.

[18] R. L. Bruun, C. S. M. García, T. B. Sørensen, N. K. Pratas, T. K. Madsen, and P. Mogensen, "Signaling design for cooperative resource allocation and its impact to reliability," 2021, *arXiv:2109.07206.*

[19] R. Zhang, X. Cheng, Q. Yao, C.-X. Wang, Y. Yang, and B. Jiao, "Interference graph-based resource-sharing schemes for vehicular networks," *IEEE Trans. Veh. Technol.*, vol. 62, no. 8, pp. 4028–4039, Oct. 2013.

[20] *Report on Hybrid ARQ Type II/III*, 3GPP, document TR 25.835 V1.0.0, Dec. 2000.

[21] *Medium Access Control (MAC) Protocol Specification*, 3GPP, document TR 25.321 V7.0.0, Dec. 2006.

[22] *Evolved Universal Terrestrial Radio Access (E-Utra) Medium Access Control (MAC) Protocol Specification*, 3GPP, document TR 36.321 V1.0.0, Dec. 2007.

[23] M. G. Sarret, D. Catania, F. Frederiksen, A. F. Cattoni, G. Berardinelli, and P. Mogensen, "Dynamic outer loop link adaptation for the 5G centimeter-wave concept," in *Proc. 21st Eur. Wireless Conf.*, 2015, pp. 1–6.

[24] A. Sampath, P. S. Kumar, and J. M. Holtzman, "On setting reverse link target SIR in a CDMA system," in *Proc. IEEE 47th Veh. Technol. Conf. Technol. Motion*, vol. 2, May 1997, pp. 929–933.

[25] C. S. M. Garcia, R. L. Bruun, T. B. Sorensen, N. K. Pratas, T. K. Madsen, J. Lianghai, and P. Mogensen, "Decentralized cooperative resource allocation with reliability at four nines," in *Proc. IEEE Global Commun. Conf. (GLOBECOM)*, Madrid, Spain, Dec. 2021, pp. 1–6.

[26] L. Hai, H. Wang, J. Wang, and Z. Tang, "HCOR: A high-throughput coding-aware opportunistic routing for inter-flow network coding in wireless mesh networks," *EURASIP J. Wireless Commun. Netw.*, vol. 2014, no. 1, p. 148, Sep. 2014, doi: 10.1186/1687-1499-2014-148.

[27] C. Fragouli, J. Y. Le Boudec, and J. Widmer, "Network coding: An instant primer," *ACM SIGCOMM Comput. Commun. Rev.*, vol. 36, no. 1, pp. 63–68, 2006, doi: 10.1145/1111322.1111337.

[28] T. Izydorczyk, M. M. Ginard, S. Svendsen, G. Berardinelli, and P. Mogensen, "Experimental evaluation of beamforming on UAVs in cellular systems," in *Proc. IEEE 92nd Veh. Technol. Conf. (VTC-Fall)*, Nov. 2020, pp. 1–5.

[29] C. Meagher, D. Hooper, C. Cirullo, J. Neff, and J.-C.-S. Chieh, "Adaptive beamforming for tele-operated unmanned ground vehicles," in *Proc. IEEE Mil. Commun. Conf.*, San Diego, CA, USA, Nov. 2013, pp. 1161–1165.

[30] M. M. Ginard, T. Izydorczyk, P. Mogensen, and G. Berardinelli, "Enhancing vehicular link performance using directional antennas at the terminal," in *Proc. IEEE Globecom Workshops (GC Wkshps)*, Dec. 2019, pp. 1–5.

[31] S. Morejon, R. Bruun, F. Fernandes, T. Sørensen, N. Pratas, T. Madsen, and P. Mogensen, "New radio sidelink with beam selection for reliable communication in high density robotic swarms," Submitted in *IEEE Veh. Technol. Conf. (VTC-Spring)*, Florence, Italy, Jun. 2023.

[32] R. Molina-Masegosa, M. Sepulcre, J. Gozalvez, F. Berens, and V. Martinez, "Empirical models for the realistic generation of cooperative awareness messages in vehicular networks," *IEEE Trans. Veh. Technol.*, vol. 69, no. 5, pp. 5713–5717, May 2020.

[33] S. Bartoletti, B. M. Masini, V. Martinez, I. Sarris, and A. Bazzi, "Impact of the generation interval on the performance of sidelink C-V2X autonomous mode," *IEEE Access*, vol. 9, pp. 35121–35135, 2021.

[34] *Medium Access Control (MAC) Protocol Specification*, 3GPP, document TS 38.321 V16.5.0, Dec. 2021.

[35] A. Bazzi, C. Campolo, A. Molinaro, A. Berthet, B. M. Masini, and A. Zanella, "On wireless blind spots in the C-V2X sidelink," *IEEE Trans. Veh. Technol.*, vol. 69, no. 8, pp. 9239–9243, Jun. 2020.

[36] *Physical Layer Procedures for Data*, 3GPP, document TS 38.214 V17.0.0, Dec. 2021.

[37] K. I. Pedersen, S. R. Khosravirad, G. Berardinelli, and F. Frederiksen, "Rethink hybrid automatic repeat request design for 5G: Five configurable enhancements," *IEEE Wireless Commun.*, vol. 24, no. 6, pp. 154–160, Dec. 2017.

[38] *Radio Resource Control (RRC) Protocol Specification (Release 16)*, 3GPP, document TR 38.331 V16.4.1, Dec. 2021.

[39] D. Chase, "Code combining—A maximum-likelihood decoding approach for combining an arbitrary number of noisy packets," *IEEE Trans. Commun.*, vol. COM-33, no. 5, pp. 385–393, May 1985.

[40] *Study on Evaluation Methodology of New Vehicle-to-Everything (V2X) Use Cases for LTE and NR*, 3GPP, document TR 37.885 V15.3.0, Jun. 2019.

[41] Y. Heng, J. G. Andrews, J. Mo, V. Va, A. Ali, B. L. Ng, and J. C. Zhang, "Six key challenges for beam management in 5.5G and 6G systems," *IEEE Commun. Mag.*, vol. 59, no. 7, pp. 74–79, Jul. 2021.

[42] M. Enescu, "Main radio interface related system procedures," in *5G New Radio a Beam-Based Air Interface*. Hoboken, NJ, USA: Wiley, 2020, pp. 297–316.

[43] *Study on Channel Model for Frequencies From 0.5 to 100 GHz*, 3GPP, document TR 38.901 V16.1.0, Dec. 2019.

[44] S.-Y. Lien, D.-J. Deng, C.-C. Lin, H.-L. Tsai, T. Chen, C. Guo, and S.-M. Cheng, "3GPP NR sidelink transmissions toward 5G V2X," *IEEE Access*, vol. 8, pp. 35368–35382, 2020. [Online]. Available: https://ieeexplore.ieee.org/document/8998153/

[45] S. Lu, J. May, and R. J. Haines, "Efficient modeling of correlated shadow fading in dense wireless multi-hop networks," in *Proc. IEEE Wireless Commun. Netw. Conf. (WCNC)*, Istanbul, Turkey, Apr. 2014, pp. 311–316.

[46] *Study of Radio Frequency (RF) and Electromagnetic Compatibility (EMC) Requirements for Active Antenna Array System (AAS) Base Station*, 3GPP, document TR 37.840 V12.1.0, Dec. 2013.

[47] *Study on 3D Channel Model for LTE*, 3GPP, document TR 36.873 V12.7.0, Dec. 2017.

[48] E. K. Al-Hussaini and A. A. M. Al-Bassiouni, "Performance of MRC diversity systems for the detection of signals with Nakagami fading," *IEEE Trans. Commun.*, vol. COM-33, no. 12, pp. 1315–1319, Dec. 1985.

[49] J. Andrews, *Fundamentals of WiMAX: Understanding Broadband Wireless Networking*. Harlow, U.K.: Prentice-Hall, 2007.

[50] S. Lagen, K. Wanuga, H. Elkotby, S. Goyal, N. Patriciello, and L. Giupponi, "New radio physical layer abstraction for system-level simulations of 5G networks," in *Proc. IEEE Int. Conf. Commun. (ICC)*, Jun. 2020, pp. 1–7.

[51] G. Pocovi, B. Soret, M. Lauridsen, K. I. Pedersen, and P. Mogensen, "Signal quality outage analysis for ultra-reliable communications in cellular networks," in *Proc. IEEE Globecom Workshops (GC Wkshps)*, Dec. 2015, pp. 1–6.

[52] A. M. Zoubir and B. Boashash, "The bootstrap and its application in signal processing," *IEEE Signal Process. Mag.*, vol. 15, no. 1, pp. 56–76, Jan. 1998.

C. SANTIAGO MOREJÓN GARCÍA (Member, IEEE) received the Engineering degree in electronics and telecommunications from the Escuela Politécnica Nacional, Ecuador, in 2012, and the M.Sc. degree in mobile communications from Telecom ParisTech/Eurecom, France, in 2017. He is currently pursuing the Ph.D. degree with the Wireless Communication Networks Section, Aalborg University, in collaboration with Nokia Standards, Aalborg, Denmark. His research interests include radio resource management and interference mitigation for decentralized networks using 3GPP sidelink.

RASMUS LIBORIUS BRUUN received the B.Sc. degree in engineering (internet technologies and computer systems) and the M.Sc. degree in engineering (networks and distributed systems) from Aalborg University, Denmark, in 2015 and 2018, respectively, where he is currently pursuing the Ph.D. degree with the Wireless Communication Networks Section, in collaboration with Nokia Standards, Aalborg, Denmark. His research interests include mobile wireless ad-hoc networks, propagation modeling, and radio resource management.

FILIPA S. S. FERNANDES (Member, IEEE) received the B.Sc. and M.Sc. degrees in electrical and computer engineering from the Instituto Superior Técnico (IST), University of Lisbon, Lisbon, Portugal, in 2016 and 2019, respectively. She is currently pursuing the Ph.D. degree with the Wireless Communication Networks Section, Aalborg University, in collaboration with Nokia Standards, Aalborg, Denmark. Her research interests include beamforming solutions for FR2 beam management and user blockage modeling in handheld devices at mmWave frequencies.

TROELS B. SØRENSEN received the M.Sc.E.E. and Ph.D. degrees in wireless communications from Aalborg University, in 1990 and 2002, respectively. He worked with type approval test methods as part of ETSI standardization activities. Since 1997, he has been at Aalborg University, where he is currently an Associate Professor with the Section for Wireless Communication Networks. He has successfully supervised more than 15 Ph.D. students, and published more than 120 journals and conference papers. His research interests include cellular network performance and evolution, radio resource management, propagation characterization, and related experimental activities.

NUNO K. PRATAS received the Licenciatura and M.Sc. degrees in electrical engineering from the Instituto Superior Tecnico, Technical University of Lisbon, Lisbon, Portugal, in 2005 and 2007, respectively, and the Ph.D. degree in wireless communications from Aalborg University, Aalborg, Denmark, in 2012. He is currently a Senior Research Specialist at Nokia. His research interests include wireless communications, networks and development of analysis tools for communication systems for 5G and 6G communications systems, in particular for sidelink use cases.

TATIANA KOZLOVA MADSEN received the Ph.D. degree in mathematics from Lomonosov Moscow State University, Russia, in 2000. Since 2001, she has been working at the Department of Electronic Systems, Aalborg University, Denmark, where she currently holds a position of an Associate Professor of wireless networking. She has been involved in a number of national and international projects developing network architectures, network protocols and solutions for intelligent transportation systems; smart grids; and automotive and train industries. Her research interests include wireless networking, including quality of service and performance optimization of converging networks, communication protocols for the IoT systems and mesh networks and methods and tools for performance evaluation of communication systems.

PREBEN MOGENSEN became a Full Professor at Aalborg University, in 2000, where he is currently leading the Wireless Communication Networks Section. He is also a Principal Scientist with the Standardization & Research Laboratory, Nokia Bell Labs. His current research interests include industrial use cases for 5G, 5G evolution, and 6G. He is a Bell Labs Fellow.

• • •